The Cluster Environment of BL Lac Objects

R. FALOMO, Osservatorio Astronomico di Padova, Italy, and
J.E. PESCE, STScI, Baltimore, U.S.A.

Introduction

BL Lac objects (hereafter BL Lacs) are an unusual kind of active galactic nuclei (AGN) which exhibit extreme properties of flux variability (large amplitude and short time scales) and polarization together with a strong non-thermal emission over a wide frequency range (e.g. Angel & Stockman 1980; Bregman 1990; Kollgaard 1994).

At variance with most of the other AGN, the optical spectra of BL Lac objects lack the strong emission lines that characterize quasars and Seyfert galaxies. This peculiar characteristic prevents an easy determination of the redshift and the discovery of BL Lacs in optical surveys. Imaging studies have shown, however, that many BL Lacs reside in the nuclei of giant elliptical galaxies, whose contribution is sometimes detectable in the optical spectra, allowing the measurement of the redshift of the sources. In contrast to the thousands of quasars that have been discovered in the last decades, the number of known BL Lacs is less than a few hundred. Only recently with X-ray surveys and/or with a combination of radio, optical and X-ray surveys has it been possible to construct sizeable and complete samples of BL Lacs (Giommi et al. 1991; Stocke et al. 1991; Stickel et al. 1991; Schachter et al. 1993).

The peculiar properties of this class of AGN are currently interpreted, in the framework of unified models, as radio galaxies with a relativistic jet which is closely aligned to the observer's line of sight. The power-law continuum and its polarization and variability together with the superluminal motion shown by many objects are all suggestive of the presence of anisotropic relativistic emission. It is also remarkable that BL Lacs (and blazars in general) are luminous γ-ray emitters (Hartman *et al.* 1993) providing model-independent support for the presence of relativistic motion in jets (Maraschi, Ghisellini, & Celotti 1992).

This hypothesis, originally proposed by Blandford and Rees (1978), implies the existence of a large number of objects intrinsically identical to the BL Lacs but with the jet pointing away from the observer. It is currently proposed that the low-luminosity (F-R I) radio galaxies (or a fraction of them) may represent the parent population of BL Lacs (e.g. Browne 1989; Urry, Padovani, & Stickel 1991; Kollgaard et al. 1992). As a test of this model one can compare unbeamed

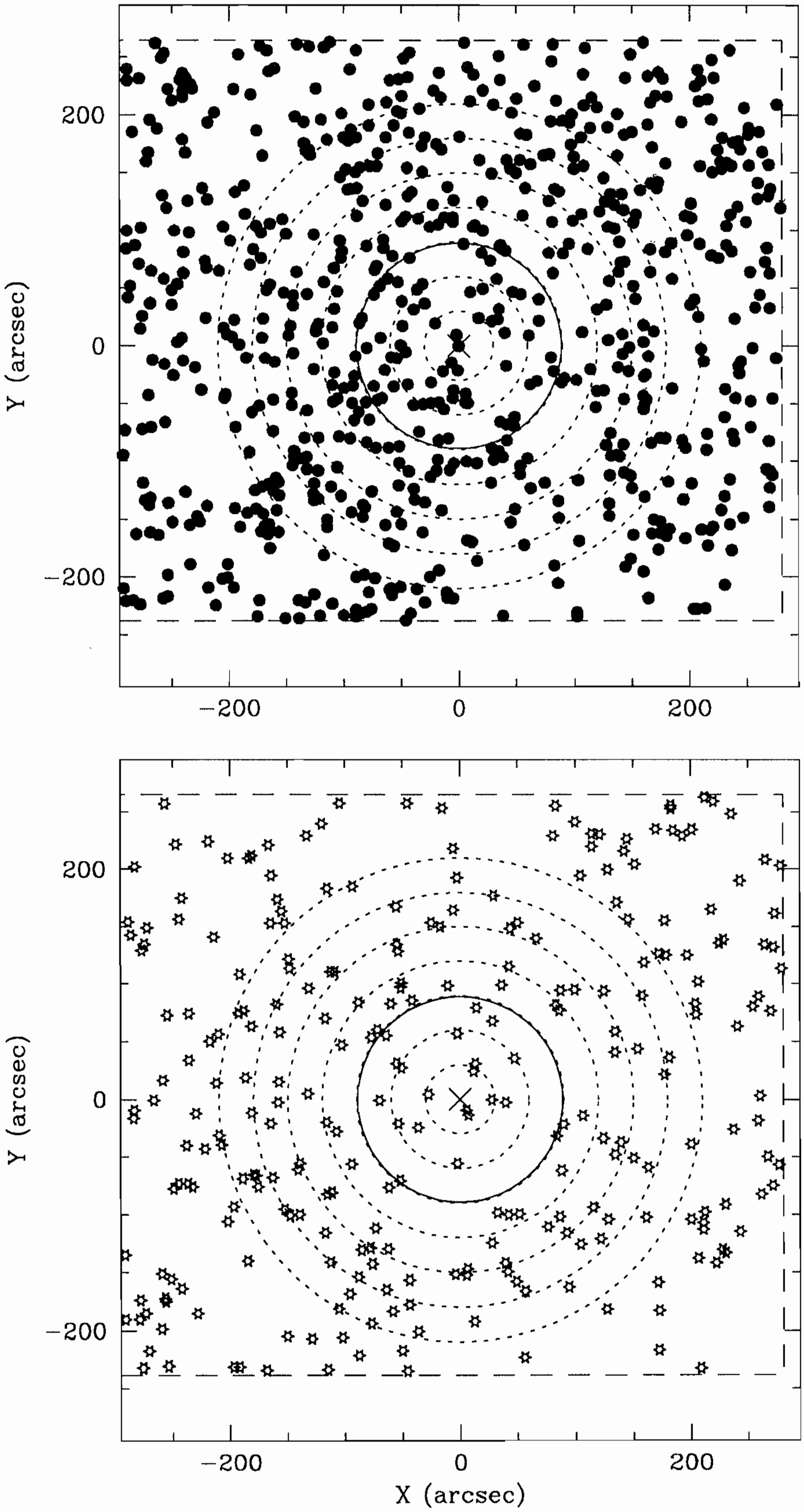

Figure 1: *Distribution of galaxies (top) and stars (bottom) in an EMMI frame (R filter 20 min) as derived from the classification obtained by FOCAS.*

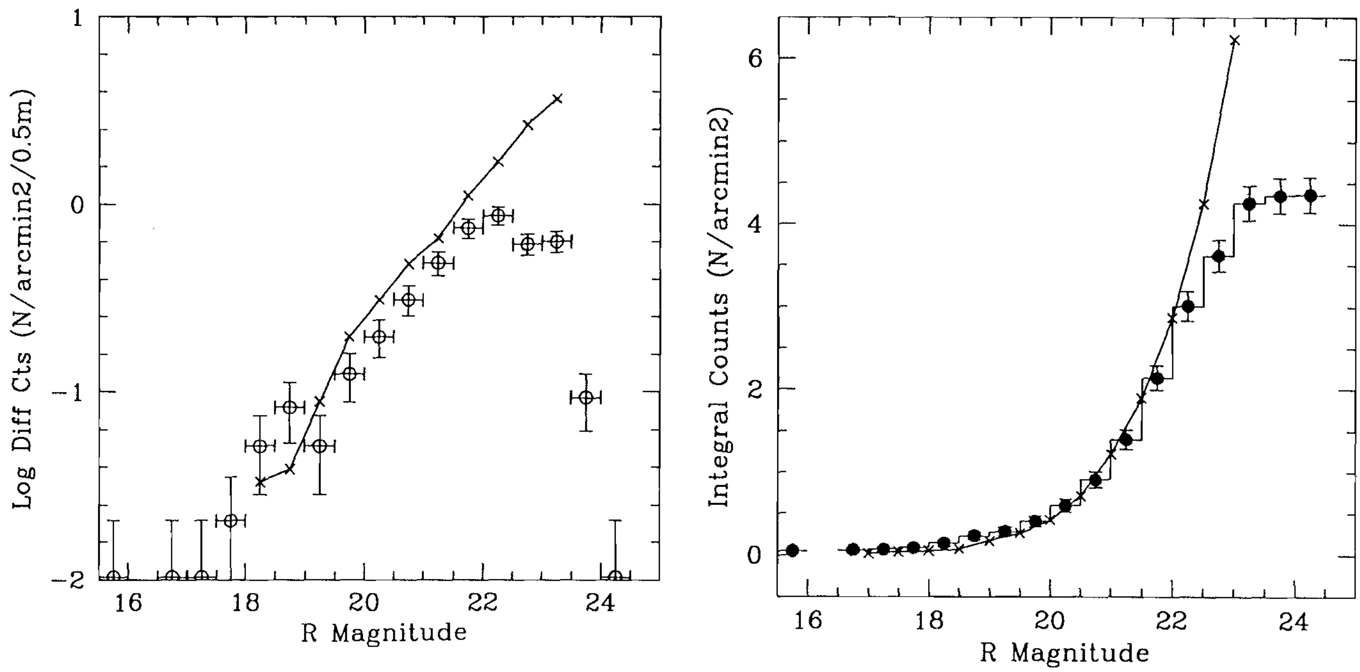

Figure 2: *The differential (left) and integral (right) galaxy counts derived from a single CCD EMMI frame (20-min exposure) compared, respectively, with counts by Metcalfe et al. (1991) and Hintzen et al. (1991) background counts.*

properties (such as extended radio emission, host galaxies and environments) of BL Lacs and parent objects or study the relative luminosity functions.

The Environment of BL Lacs

The study of the environment of BL Lac objects may be a useful tool for understanding the BL Lac phenomena. It gives clues to the role played by the environment for triggering and fuelling the activity in elliptical galaxies and in particular may help to enlighten the relationship between BL Lacs and their parent population.

Contrary to the case of quasars, the study of the environs of BL Lacs is complicated by the faintness of their spectral lines with respect to the continuum, hindering the derivation of redshifts and, thus, the proof of physical association with nearby galaxies.

Until recently only a few studies have been conducted on the cluster environment of BL Lacs (Disney 1974; Craine, Tapia, & Tarenghi 1975; Butcher *et al.* 1976; Fosbury & Disney 1976; Ulrich 1978). These investigations generally failed to provide clear evidence of a physical association and it was suggested that BL Lacs may avoid cluster environments (Weistrop *et al.* 1981).

The use of modern instrumentation on large optical telescopes enabled the study of BL Lac environments in a much more effective way. For more than half of the known BL Lacs the redshift has been determined either from weak absorption lines of the host galaxy or from intervening absorption lines that give a lower limit to it. On the imaging front the capability to detect and classify galaxies over a large field of view is now easily achievable.

Here we present a summary of the results obtained from a programme undertaken at La Silla to investigate the environments of BL Lacs and outline the analysis procedure adopted. To date we have observed $\sim$ 20 targets that are a mixture of radio- and X-ray selected objects.

The capability of NTT to change the instrument configuration during the same observing night also enabled us to obtain high-resolution images with SUSI in order to study the close environment and host galaxy properties for a number of BL Lacs. Here, however, we concentrate on the large-scale environment.

Observations and Data Analysis

We used the ESO NTT operated both at La Silla and via remote control from Garching to obtain images and spectra of the fields around BL Lacs. Conditions were photometric and seeing (FWHM), as measured on the CCD frames, ranged from 0.7 to 1.5 arcsec for most of the data obtained. We obtained pairs of images of the fields around BL Lacs using EMMI in the R filter with typical exposure times of 2 and 20 minutes. The EMMI images cover a useful field of 7.5 $\times$ 7.5 arcmin^2 at a scale of 0.44 arcsec pixel^{-1} (TH 1024 $\times$ 1024 pixels; pixel size 19 μm) or 9.7 $\times$ 8.5 arcmin^2 at a scale of 0.35 arcsec pixel^{-1} (1660 $\times$ 1450 pixels) depending on the CCD used. This corresponds to 0.5–4 Mpc^2 for objects at z = 0.07–0.6 (we assume H_0 = 50 km s^{-1} Mpc^{-1} and q_0 = 0.5 throughout).

After reduction of images using procedures available in the Image Reduction and Analysis Facility (IRAF; bias subtraction, trimming, flat fielding), cosmetic defects such as saturated rows and columns were cleaned. In certain cases, some saturated stars were removed as these were found to cause problems in a later phase of the analysis. We also removed all detectable cosmic-rays using the IRAF task COSMICRAYS.

In addition to direct images, we obtained spectra of some of the galaxies in the field of BL Lacs for a selected number of objects. A long slit (2″ wide) was oriented in such a way as to secure at least two objects at a time. For all spectra, we employed a grism of 300 gr mm^{-1} giving a dispersion of 246 Å mm^{-1} in the range 4000 to 8000 Å. Spectra were wavelength calibrated using an HeAr lamp, and relative flux calibration was derived from observations of standard stars (Stone 1977).

Classification of Objects

Because we want to study the distribution of the galaxies around our programme objects, the most important part of the analysis involves the detection and classification of objects in each image. To detect and classify objects (as stars, galaxies, or noise) we adopted the Faint Object Classification and Analysis Software (FOCAS), developed by Jarvis & Tyson (1981), revised and expanded by

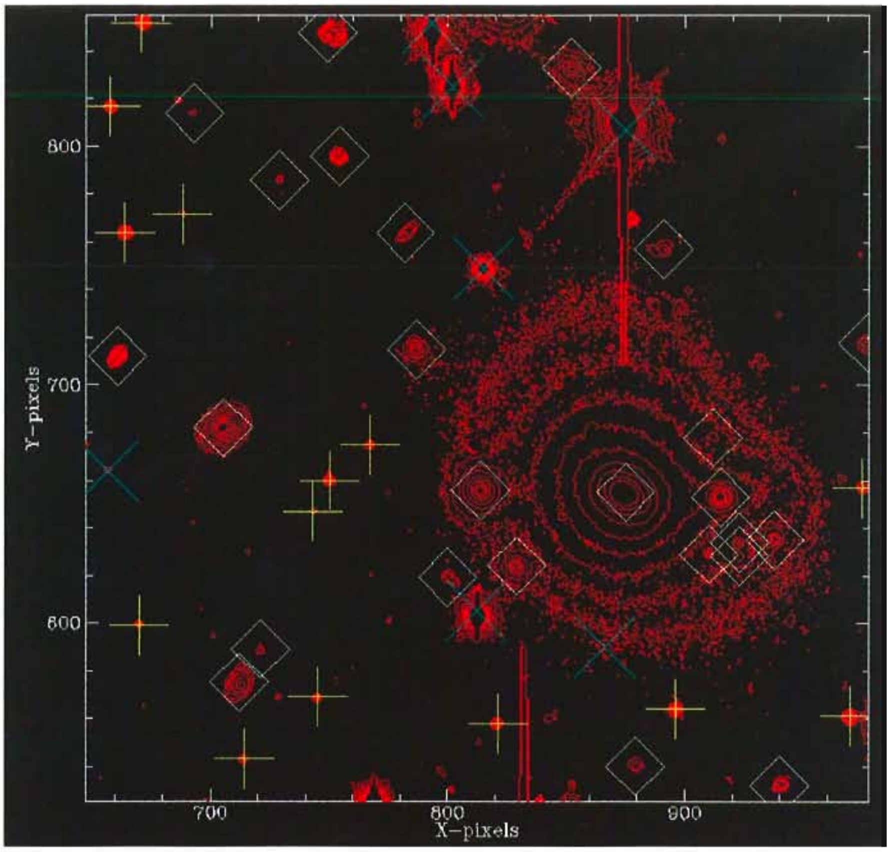

Figure 3: *Contour plot of a portion of an EMMI CCD frame with superposed the classified objects (◇ galaxies, + stars, × defects or saturated stars).*

Francisco Valdes of the National Optical Astronomy Observatories.

Classification of the objects is based on a comparison of their shape with the point spread function (PSF) determined from many (usually more than 20) stars in the field. Standard classification templates were used following Hintzen *et al.* (1991). For images taken under good conditions, the total number of objects classified can be more that 600 for a typical 20-minute exposure (see example in Fig. 1).

Objects were detected and classified up to the magnitude limit (usually R = 22–23 for a good-quality, 20-minute exposure) for each image. These limits were determined from the peaks of the differential number-count distribution of galaxies (see Fig. 2). Above this limit it becomes difficult to distinguish galaxies from stars with the automatic detection algorithm of FOCAS. Catalogues of objects detected were created for each image. The automatic classification can be checked by manual inspection of random objects all over the image. This however requires a considerable amount of time.

In order to speed up the process of checking the identified objects, we combined more catalogues (e.g., derived with different exposure times or conditions) of the same field. To allow an immediate visualization of results, we implemented a set of procedures using the SuperMongo command language. These include contour plots of the field with all classified objects identified (see Fig. 3) and a number of interactive tools to look at the distribution of galaxies (and stars) in the catalogue (see Fig. 1) and its behaviour as a function of the magnitude (see Fig. 4).

This was extremely useful in providing rapid feedback with the output catalogues derived from the FOCAS analysis. After adjusting the critical parameters (e.g., minimum image size for detection, sigma above and below the sky for detection) the FOCAS classifications appear accurate for about 90% of the objects. As a general remark we found that 20–50% of the objects can be missclassified if they are at the faintest flux levels (near the magnitude limit) or if images obtained under poor seeing conditions ($\gtrsim 1.7''$).

Results

Our investigation of BL Lac environments has provided clear evidence that, contrary to previous suggestions, BL Lacs are often located in regions of higher than average galaxy density. This is estimated by studying the density distribution of galaxies as a function of the distance from the BL Lac object and computing the angular and spatial cross-correlation functions. For about 10 objects of known redshift we obtained spectra of 1 to 5 galaxies in the field and found that these galaxies are physically associated with the BL Lac objects.

The richness of the cluster may be estimated using the number, $N_{0.5}$, of excess galaxies with $m \leq m_3 + 2$ (where m_3 is the third-ranked cluster galaxy, projected within a 0.5 Mpc radius of the cluster centre. This parameter is related to N_R, the number of galaxies within the standard Abell radius (3 Mpc; Abell 1958) of the cluster centre by the empirical relation: $N_R = 3.3 N_{0.5}$ (Bahcall 1981).

As an example we report the case of the bright ($m_V \approx 12.5$) BL Lac object PKS 2155–304 at z = 0.116. This is an extensively studied object at every frequency (e.g., Treves *et al.* 1989 and references therein). Our imaging and spectroscopic study shows that the BL Lac is hosted by a giant elliptical galaxy of $M_V \sim -22.5$ which is the dominant member of a poor cluster of galaxies (see Fig. 5). The host galaxy has two faint companion galaxies (G1 and G2) at projected distances less than 50 Kpc at the same redshift as PKS 2155–304. Moreover, a more conspicuous ($M_V = -21.4$) galaxy (G4), still at the same redshift, is located $\sim 113''$ south of the BL Lac object, corresponding to a projected distance of ~ 300 kpc. This galaxy is itself surrounded by faint companions. The richness of the cluster derived from galaxy counts yields an Abell richness class of about 0 (see Falomo, Pesce, & Treves 1993 for more details).

From our study we found that, on average, BL Lacs are associated with poor

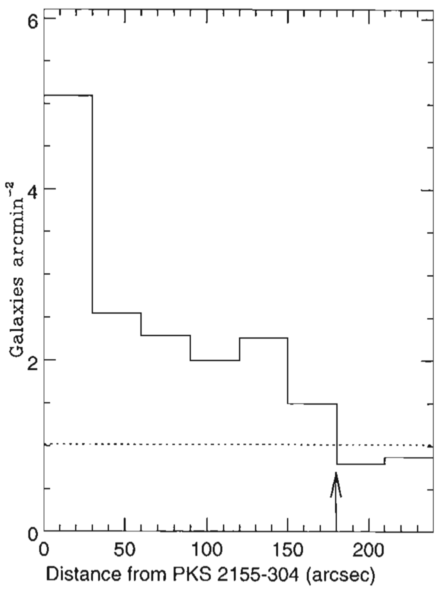

Figure 4: *Density distribution of galaxies as a function of the distance from the BL Lac object PKS 2155–304. The arrow marks the distance corresponding to 0.5 Mpc radius.*

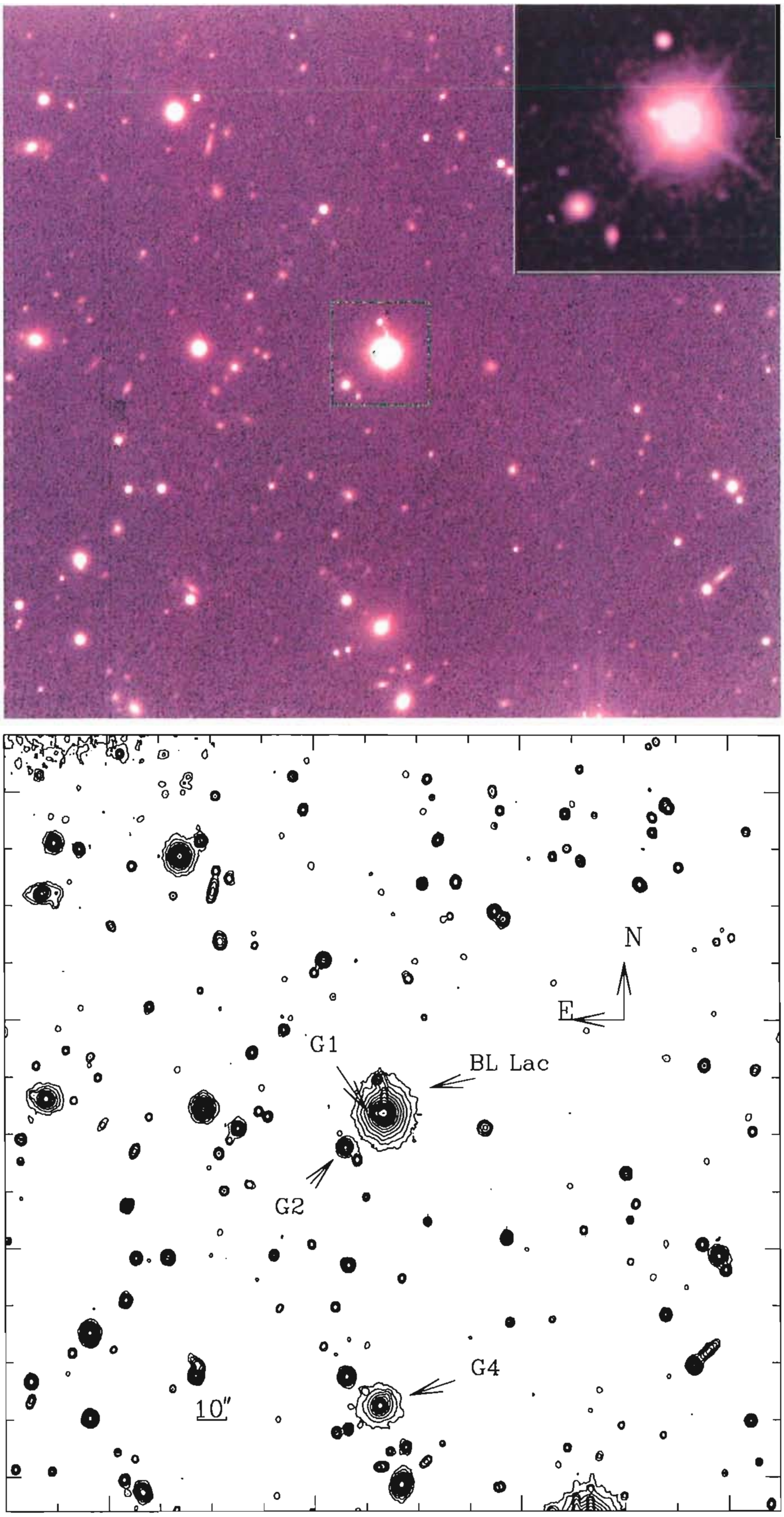

Figure 5: *(Top) The central part (2.5′ × 2.5′) of the field of the bright PKS 2155–304 (EMMI R filter 20 min). The BL Lac object (at the centre) is here clearly saturated. North is up and east to the left. The inset shows the immediate environments as imaged with SUSI (R filter 5 min) under sub-arcsec seeing conditions. This image has been deconvolved using the Richardson-Lucy algorithm. (Bottom) Contour plot of the field with main objects labelled.*

clusters of galaxies (Abell richness class ∼ 0). However, some cases of association with medium rich clusters exist.

Objects in Rich Environments

One interesting BL Lac object in a rich environment is PKS 0548–322. This is a bright (m_V = 15.5) and nearby BL Lac object for which the association with a cluster of galaxies at z ∼ 0.04 was suggested (Disney 1974). The hypothesis was, however, soon ruled out by the measurement of the redshift (z = 0.069) of PKS 0548–322 (Fosbury & Disney 1976).

Our images (see Fig. 6) clearly show an enhancement of galaxies around the source within 0.5 Mpc of projected distance from PKS 0548–322. Spectroscopy of five of the galaxies in this field (G1, G2, G4, G5, G6) confirm they form a cluster of galaxies physically associated with the BL Lac object. The host galaxy of PKS 0548–322 is a giant elliptical of M_V = –23.4 and is likely the dominant member of the cluster. Moreover, it has a pair of companion galaxies at projected distance < 40 Kpc, with a clear signature of tidal interactions. Our estimate of the richness of the cluster yields $N_{0.5}$ = 29 corresponding to Abell richness class 2 (see Falomo, Pesce, & Treves 1994 for more details).

Another interesting case is represented by the X-ray selected BL Lac H 0414+009. This is a relatively more distant object (z = 0.287) that is also embedded in a luminous (M_V ∼ –23.5) elliptical galaxy (Falomo & Tanzi 1991). H 0414+009 (see Fig. 7) is surrounded by many faint galaxies exhibiting a peculiar disposition (Falomo, Tanzi, & Treves 1991). The clustering of the galaxies around the object suggests they form a loose group, with some of the galaxies forming pairs. The excess of galaxies within 0.5 Mpc with respect to the average galaxy density is quite clear. We found 29 galaxies down to the magnitude limit of m_R = 21.5 while a total of 14.4 ± 3.8 is expected from average counts. Spectroscopy of three of the galaxies confirm their physical association while one appears to be a foreground object. Moreover, the redshifts of galaxies A1 and A2 are identical within the errors, confirming that they form a physical pair. The richness parameter estimated from $N_{0.5}$ yields an Abell richness of class 0. (See McHardy *et al.* 1992 and Falomo, Pesce, & Treves 1993 for more details).

Conclusions

Our ongoing study of BL Lac environmental properties has shown that BL Lacs are indeed found in regions of enhanced galaxy density. They seem to

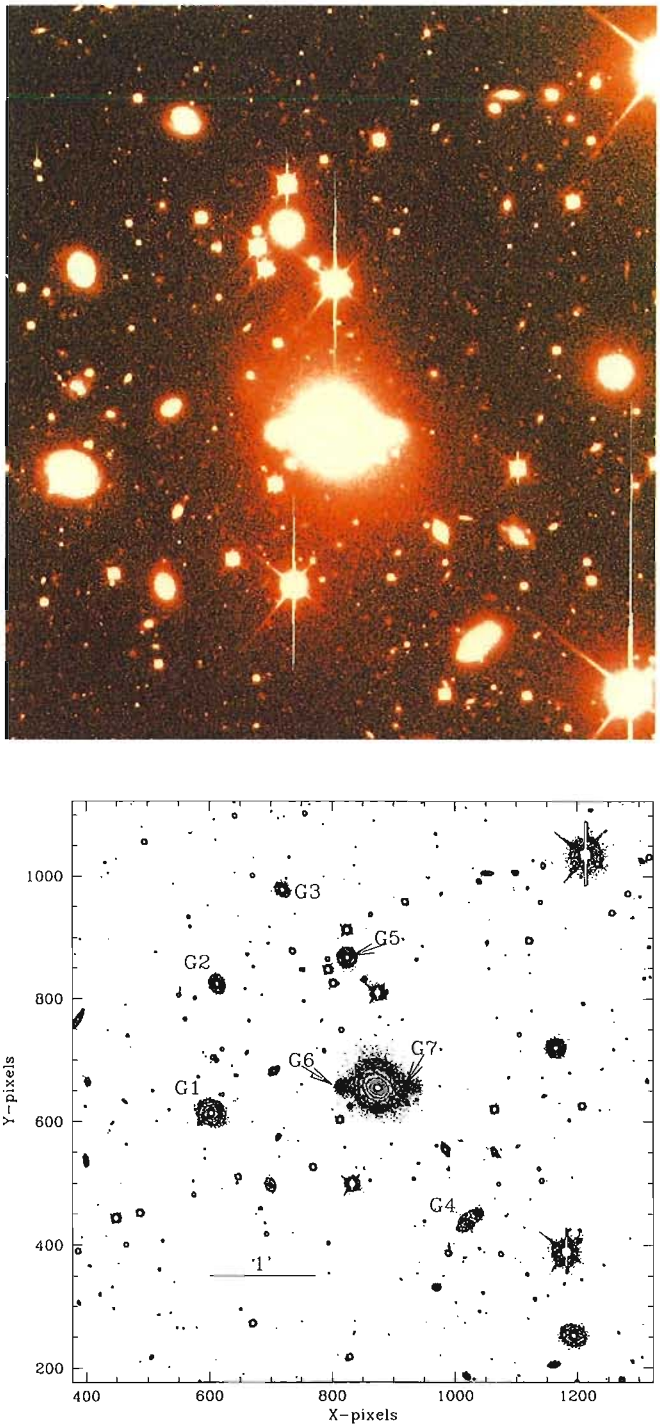

Figure 6: *(Top) The central part (4′ × 4.5′) of the field of PKS 0548–32 (EMMI R filter 20 min). North is up and east to the left. The BL Lac (main object at centre) is surrounded by a group of galaxies at the same redshift as the giant elliptical hosting 0548–322. (Bottom) Contour plot of the field with main objects labelled.*

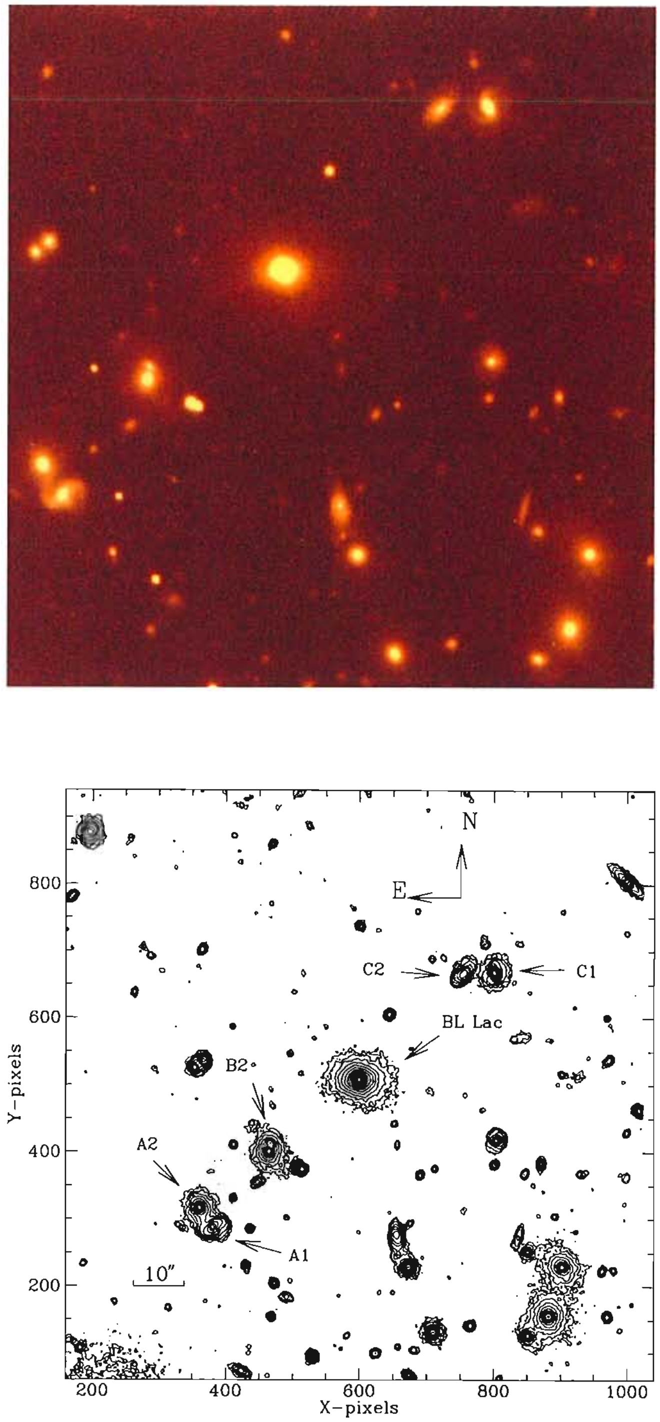

Figure 7: *(Top) The field (1.4′ × 1.5′) around the X-ray BL Lac (z = 0.287) H0414+004 (SUSI R filter 20 min). North is up and east to the left. The BL Lac (brightest object near the centre) is clearly in a cluster of galaxies with some of them forming pairs. (Bottom) Contour plot of the field with main objects labelled.*

prefer groups or poor (Abell richness class 0) clusters. We found that on average $N_{0.5}$ = 6 ± 4. While some individual BL Lacs are found in rich clusters, these seem to be a small minority.

From the 18 objects so far investigated (about 50% of our whole sample) we derived an average amplitude of the angular correlation function (BL Lac – galaxies) A_{bg} normalized to the general galaxy–galaxy amplitude A_{gg} of $< A_{bg}/A_{gg} >$ = 7 ± 4. This value is very similar to what is found in the case of radio loud quasars (see e.g. Hartwick and Schade 1990 and references therein).

Because the properties of the BL Lac environments are not dependent on orientation effects, they may be a useful tool to test the beaming model, by comparison with the environmental properties of the proposed BL Lac parent population. Although the properties of the environments of F-R I class radio galaxies may be somewhat different depending on the sample considered (e.g., Prestage & Peacock 1988, 1989; Yates, Miller, & Peacock 1989; Hill & Lilly 1991), they appear consistent with that derived for BL Lac objects based on the present data. The average value of $N_{0.5}$ for F-R

I radio galaxies derived combining available samples (see Pesce 1993) yields $<N_{0.5}>_{FRI} = 7.1 \pm 8$. The large scatter being due in part to differences of samples and redshift distribution.

We note also that F-R I radio galaxies represent an heterogeneous class and it is possible that the parent objects of BL Lacs form a subset of F-R I galaxies.

Objects in our sample are a mixture of radio selected and X-ray selected targets (corresponding to radio-strong and radio-weak emitters). Although a number of different emission properties are found to characterize these subclasses (see e.g. Giommi *et al.* 1994), we do not find systematic differences of environment between the two.

Our results are consistent with what is being found by other similar studies. Wurtz *et al.* (1993) and Smith *et al.* (1995) have concentrated on X-ray selected BL Lac objects while Stickel *et al.* (1993) and Fried *et al.* (1993) have studied some of the radio selected BL Lacs. In most cases, the clusters found are relatively poor (Abell richness class 0-1) with a few objects in richer environments.

If BL Lacs are aligned versions of low-luminosity (F-R I) radio galaxies, it might be expected that Flat Spectrum Radio Quasars (FSRQs), which share many of the properties of BL Lacs but have strong and broad emission lines, are aligned examples of high-luminosity (F-R II) radio galaxies. We point out that a detailed comparison of environmental and host properties of BL Lacs and F-R I galaxies with FSRQs and F-R II radio galaxies would help to constrain the proposed unified schemes of AGN.

Acknowledgement

We thank A. Treves for useful suggestions to this manuscript. J.E.P. and work on BL Lac environments at STScI are supported by NASA grants NAG5-1034 and NAG5-2154.

References

Abell, G. O., 1958, *ApJS*, **3**, 211.
Angel, J. R. P., & Stockman, H. S., 1980, *ARAA*, **18**, 321.
Bahcall, N. A. 1981, *ApJ*, **247**, 787.
Blandford, R. D., & Rees, M. J. 1978, in Pitts. Conference on BL Lac Objects, ed. A. N. Wolfe (Univ. of Pitts. Press), 328.
Bregman, J. P., 1990, *A&AR*, **2**, 125.
Browne, I. W. A. 1983, *MNRAS*, **204**, 23.
Butcher, H. R., *et al.* 1976, *ApJ*, **209**, L11.
Craine, E. R., Tapia, S., & Tarenghi, M., 1975, *Nature*, **258**, 56.
Disney, M. J., 1974, *ApJL*, **193**, L103.
Falomo, R., Pesce, J. E., & Treves, A., 1993, *AJ*, **105**, 2031.
Falomo, R., Pesce, J. E., & Treves, A. 1994, *ApJ Letters*, in press.
Falomo, R., & Tanzi, E. G., 1991, *AJ*, **102**, 1294.
Falomo, R., Tanzi, E. G., & Treves, A., 1991, *A&A*, **249**, 341.
Fosbury, R. A. E., & Disney, M. J., 1976, *ApJL*, **207**, L75.
Fried, J. W., Stickel, M., & Kühr, H., 1993, *A&A*, **268**, 53.
Giommi, P., *et al.* 1991, *ApJ*, **378**, 77.
Giommi, P., Ansari, S. and Micol, A. 1994, *A&ASS*, in press.
Hartwick, F.D.A. and Schade, D. 1990, *Ann. Rev. Astr. Astrophys.* **28**, 437.
Hartman, R., *et al.* 1993, in Proc. of the 2nd Compton Symposium, College Park, MD, Sept. 1993, in press.
Hill, G. J., & Lilly, S. J., 1991, *ApJ*, **367**, 1.
Hintzen, P., Romanishin, W., & Valdes, F., 1991, *ApJ*, **366**, 7.
Jarvis, J. F., & Tyson, J. A., 1981, *AJ*, **86**, 476.
Kollgaard, R. I., *et al.* 1992, *AJ*, **104**, 1687.
Kollgaard, R. I 1994, *Vistas in Astronomy*, **38**, 29.
Maraschi, L., Ghisellini, G., & Celotti, A., 1992, *ApJ*, **397**, L5.
McHardy, I. M., Luppino, G. A., George, I. M., Abraham, R. G., & Cooke, B. A., 1992, *MNRAS*, **256**, 655.
Metcalfe, N., Shanks, T., Fong, R., & Jones, L. R., 1991, *MNRAS*, **249**, 498.
Pesce, J. E 1993, PhD Thesis.
Prestage, R. M., & Peacock, J. A., 1988, *MNRAS*, **230**, 131.
Prestage, R. M., & Peacock, J. A., 1989, *MNRAS*, **236**, 959.
Schachter, J. F., *et al.* 1993 *ApJ*, **412**, 541.
Smith, E. P., O'Dea, C. P., & Baum, S. A., 1995, *ApJ*, in press.
Stickel, M., *et al.* 1991, *ApJ*, **374**, 431.
Stickel, M., Fried, J. W., & Kühr, H. 1993, A&AS, 98, 393.
Stocke, J. T., *et al.* 1991, *ApJS*, **76**, 813.
Stone, R. P. S., 1977, *ApJ*, **218**, 767.
Treves, A., *et al.* 1989, *ApJ*, **341**, 733.
Ulrich, M.-H. 1978, *ApJ*, **222**, L3.
Urry, C. M., Padovani, P., & Stickel, M. 1991, *ApJ*, **382**, 501.
Weistrop, D., *et al.* 1981, *ApJ*, **249**, 3.
Wurtz, R., Ellingson, E., Stocke, J. T., & Yee, H. K. C., 1993, *AJ*, **106**, 869.
Yates, M. G., Miller, L., & Peacock, J. A., 1989, *MNRAS*, **240**, 129.

COME-ON+ Adaptive Optics Images of the Pre-Main Sequence Binary NX Pup

E. TESSIER[1], *J. BOUVIER*[2], *J.-L. BEUZIT*[3,5] *and W. BRANDNER*[4,5]

[1]*Royal Greenwich Observatory, Cambridge, England;* [2]*Observatoire de Grenoble, Université Joseph Fourier, France;* [3]*Observatoire de Paris, Section de Meudon, France;* [4]*Astronomisches Institut der Universität Würzburg, Germany;* [5]*ESO-La Silla*

Introduction

Using adaptive optics (AO) at the ESO 3.6-m telescope, we obtained diffraction limited JHK images of the region around the Herbig AeBe star NX Pup. NX Pup is resolved as a close binary with a separation of 0.128″ (the binary nature of NX Pup was originally discovered by HST) that we refer to as NX Pup AB; a third component NX Pup C is found at a distance of 7.0″ and is classified as a classical T Tauri star. We first describe the procedure that we followed in order to extract the maximum information from the AO images. We then discuss the evolutionary status of the NX Pup system on the basis of its IR properties derived from the AO images, as well as from the visual photometry and spectroscopy subsequently obtained at ESO.

AO Observations

We used the ESO adaptive optics system ComeOn+ (CO+), which was developed in collaboration by the Observatoire de Paris, ONERA, ESO, Laserdot and LEP, in combination with the SHARP II (System for High Angular Resolution Pictures) camera from the Max-Planck Institute for Extraterrestrial Physics (MPE). See Beuzit *et al.* 1994, *The Messenger* 75, 33 and references therein for a description of the CO+ system. The SHARP II camera is equipped with a Rockwell NICMOS-3 array. The image scale was 0.050″/pixel giving a field size of 13″× 13″. We observed NX Pup on